Research and Application of Dynamic Anti-Deviation Mechanism of Pre-Bent Drill Assembly in Complex Offshore Formations

Wenlong Li , Zhuangwei Li , Jiangjun Xi , Nan Jin , Long Cheng , Guoliang Zhu , Xingpeng Zhang , Shuzhan Li *

Posted Date: 14 April 2026

doi: 10.20944/preprints202604.0936.v1

Keywords: pre-bent; anti-deviation; exploration drilling; drilling acceleration

 doi:10.20944/preprints202604.0936.v1

Article

Research and Application of Dynamic Anti-Deviation Mechanism of Pre-Bent Drill Assembly in Complex Offshore Formations

Wenlong Li [1], Zhuangwei Li [1], Jiangjun Xi [1], Nan Jin [1], Long Cheng [1], Guoliang Zhu [2], Xingpeng Zhang [3] and Shuzhan Li [3,*]

[1] Tianjin Branch of CNOOC Ltd., Tianjin 300459, China
[2] China University of Petroleum (Beijing), Beijing 102200, China
[3] School of Marine Technology and Equipment, Hainan University, Haikou 570228, China
* Correspondence: 996720@hainanuedu.cn; Tel.: +8613121103729

Abstract

During the exploration drilling process, maintaining a vertical well trajectory is a critical issue. In geological formations with complex conditions that are prone to well deviation, conventional drilling tool assemblies exhibit poor anti-deviation performance. To achieve anti-deviation and accelerate drilling in exploration wells, a pre-bent drilling tool assembly is proposed. In this study, a dynamic model of the pre-bent drilling tool assembly was established. The anti-deviation mechanism of the pre-bent drilling tool assembly was investigated. The deviation-reduction effects of the drilling tool assembly under different parameter conditions were analyzed. The results indicate that the deviation-reducing force initially increases and then decreases as the pre-bend angle of the anti-deviation drilling tool increases. When the bend angle is between 1° and 1.13°, a larger deviation-reducing force is generated at the drill bit. A shorter distance (L_1) between the near-bit stabilizer and the drill bit, a smaller near-bit stabilizer diameter, and a larger upper stabilizer diameter result in a greater deviation-reducing force. The relationship between the deviation-reducing force and the distance between the two stabilizers (L_2) is not explicitly linear, but a decreasing trend is observed after the distance exceeds 10 m. Compared with the conventional pendulum anti-deviation drilling tool assembly, the deviation-reducing force of the pre-bent drilling tool assembly has an advantage of more than two orders of magnitude. Based on the calculation results, the optimal design of the pre-bent drilling tool assembly was carried out. The bend angle was increased to 1.15°, the diameter of the near-bit stabilizer was reduced to 305 mm, L2 was reduced to 9–11 m, and L1 was reduced to 0.9 m. Field applications in 22 exploration wells show that the pre-bent drilling tool assembly provides excellent anti-deviation effects. It can fully release the weight on bit while ensuring a vertical trajectory, achieving a 14% increase in the drilling rate. This technology effectively replaces vertical steering tools. Tool costs are significantly saved, providing an effective method for anti-deviation in complex formations.

Keywords: pre-bent; anti-deviation; exploration drilling; drilling acceleration

0. Introduction

In the oil and gas industry, vertical wellbores are commonly used for exploration drilling. In recent years, deep formations have become the primary focus for oil and gas exploration discoveries in the Bohai Oilfield, the largest offshore oilfield in China[1,2]. However, the geological conditions of deep formations in the Bohai Sea are complex. The formation dip is large, and the heterogeneity is strong[3,4], which leads to prominent well deviation problems. Furthermore, high weight on bit during the drilling of deep formations can also cause the drill string to bend. This results in an increasing inclination angle of the drill bit, causing the well deviation tendency to become

 doi:10.20944/preprints202604.0936.v1

increasingly severe[5,6]. In a certain block of the Bohai Sea, well deviation occurred in 7 exploration wells (Figure 1). The deviation angles ranged from 4.51° to 36.55°. A significant increase in the deviation angle is observed, especially as the well depth increases.

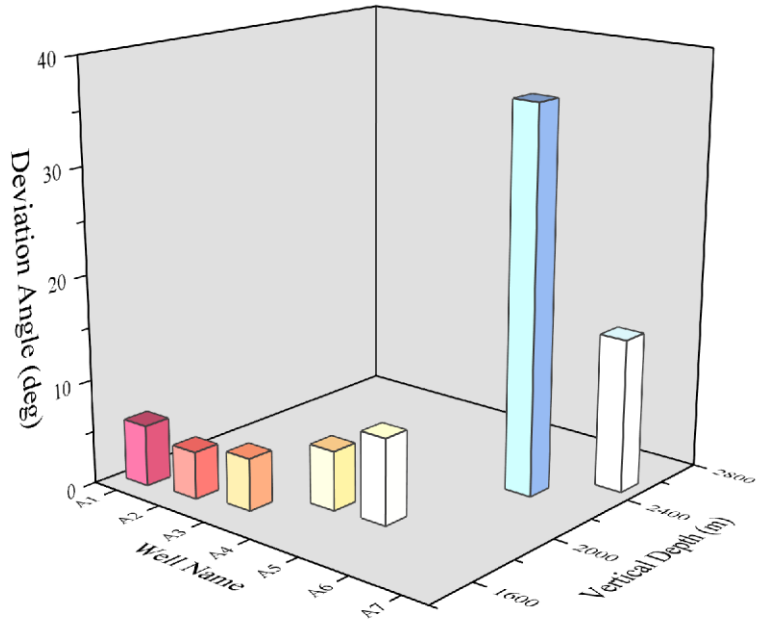

Figure 1. Distribution of deviation angles in 7 exploration wells in a certain block of the Bohai Sea.

Well deviation is a common risk issue in drilling engineering. It persists throughout the processes of drilling, completion, and subsequent oil and gas testing. A series of hazards are generated, directly affecting engineering safety, reserve evaluation, and development plan formulation[7,8]. The core objective of drilling is to accurately penetrate oil and gas reservoirs (target layers). The hit effect on the target layer is directly impacted by well deviation. Reservoirs might be missed, or the reservoir penetration rate might be insufficient[9]. Secondly, well deviation is often accompanied by irregular wellbores, such as excessive dogleg severity. Various downhole accidents can be easily induced. In severe cases, wellbore abandonment or casualties may result. Meanwhile, a vertical wellbore is the foundation for subsequent cementing, completion, and oil and gas testing. Substandard cementing quality and difficulties in running completion and testing tools are caused by irregular wellbores. Furthermore, to correct well deviation, repeated tripping operations and drill string replacements are required. Additional consumables such as drill pipes, casings, and drilling fluid must be utilized. The operation time for a single well is extended, and equipment and labor costs rise significantly[10].

To prevent significant deviation of the wellbore from the target, there are specific standards for the inclination of vertical wells. However, under the combined effects of various factors such as steep formation dips, strong formation heterogeneity, and unsuitable drill string configurations, an increasing trend in well inclination is observed. This is also impacted by the tendency of the drill bit to deviate towards softer formations and avoid harder ones[11–13]. To ensure the verticality of wellbores, anti-deviation drill string assemblies and automatic vertical drilling tools are commonly utilized. Popular anti-deviation assemblies include pendulum assemblies, full-gauge assemblies, steep angle anti-deviation assemblies, and tower assemblies[14–16].

However, specific limitations are found when most of these assemblies are used. For instance, pendulum assemblies can only be used with light pressing and lifting techniques. Drilling speeds can be slowed down by this due to low drilling pressures. Full-gauge assemblies are not suitable for layers prone to deviation or collapse. Steep angle assemblies require a specific initial well inclination. Thus, in complex formations, conventional anti-deviation combinations may not meet the requirements for controlling well deviation and increasing drilling speed. Automatic vertical drilling tools refer to vertical guidance tools. Tools such as Power V are commonly included, which are

 doi:10.20944/preprints202604.0936.v1

categorized into directional and pushing types. However, these vertical guidance drilling tools are costly to operate and have specific requirements for wellbore sizes. They are made less suitable for unconventional standard-sized wellholes.

Field engineers have discovered that a combination drilling with a sliding steerable drill assembly featuring a single bent screw can maintain good verticality in a straight hole[17,18]. However, its anti-deviation mechanism has not been clearly understood. The influence of various structural parameters on the anti-deviation effect is also unclear. In this paper, a dynamic model for a pre-bent drill string assembly has been developed. Through computational analysis, the impact of various structural parameters on the deflection reduction capability of the pre-bent structure was determined. This led to the optimization of an efficient anti-deviation drill string combination. Field applications have demonstrated that this combination not only effectively prevents deviation but also enhances drilling speed. It is proven to be of great value for widespread application.

1. BHA Dynamic Model

1.1. Construction of the Mechanical Model

The bottom hole assembly (BHA) can be treated as a slender Euler beam situated in a three-dimensional curved wellbore. In the three-dimensional wellbore, spatial bending deformation is generated under the effects of self-weight, weight on bit, torque, wellbore constraints, and drilling fluid pressure. This spatial bending deformation[19] is illustrated in Figure 2.

To conform to practical conditions and facilitate research, several basic assumptions are adopted:

(1)The rod-pipe string is in a state of linear elastic deformation.

(2)The cross-section of the rod-pipe string is circular or annular.

(3)The influence of shear force on the deformation of the rod-pipe string is neglected.

The tangential vector on the BHA is defined as:

$$\boldsymbol{e}_t = \frac{\partial \boldsymbol{r}}{\partial l} \tag{1}$$

Where $\boldsymbol{e}_t$ is the tangential vector along the BHA axis; $\boldsymbol{r}$ is the BHA displacement ; and l is the BHA distance.

Since

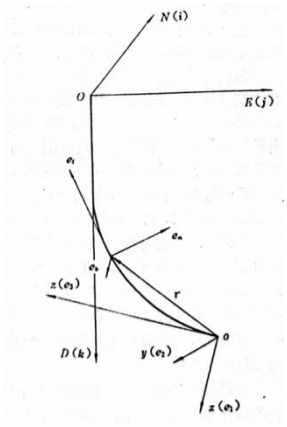

Figure 2. 3D mechanical model of downhole drilling tools

$$U\boldsymbol{e}_1 + V\boldsymbol{e}_2 + W\boldsymbol{e}_3 \tag{2}$$

Then

 doi:10.20944/preprints202604.0936.v1

$$\boldsymbol{e}_t = \frac{\partial U}{\partial l}\boldsymbol{e}_1 + \frac{\partial V}{\partial l}\boldsymbol{e}_2 + \frac{\partial W}{\partial l}\boldsymbol{e}_3 \tag{3}$$

Where, U is the coordinate in the x-direction of the point on the BHA axis; V is the coordinate in the y-direction; W is its coordinate in the z-direction. e_1, e_2, e_3 are the unit vectors of the coordinate axes, respectively.

The internal force vector of the microelement section (Figure 3) is expressed as:

$$\boldsymbol{F} = F_x\boldsymbol{e}_1 + F_y\boldsymbol{e}_2 + F_z\boldsymbol{e}_3 \tag{4}$$

Where: *F* is the internal force vector of the microelement section; *Fx*,*Fy*,*Fz* are the components of the internal force in the x, y, and z directions, respectively.

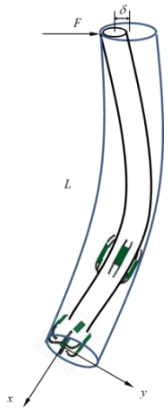

Figure 3. Schematic diagram of spatial deformation of BHA

For the BHA microelement section, the physical equation is expressed as:

$$M = EI(e_t \times \frac{\partial e_t}{\partial l}) + M_t e_t \tag{5}$$

Where: M is the bending moment vector of the BHA microelement section; EI is the bending stiffness of the BHA; M_t is the torque vector of the BHA microelement section; $\boldsymbol{M}_t = GJ\frac{\partial \boldsymbol{\gamma}}{\partial l}$, GJ is the torsional stiffness; $\boldsymbol{\gamma}$ is the torsion angle.

By substituting Equation (3) and Equation (4) into Equation (5), the following equation is obtained:

$$\begin{aligned} M = EI[&(\frac{\partial V}{\partial l}\frac{\partial^2 W}{\partial l^2} - \frac{\partial W}{\partial l}\frac{\partial^2 V}{\partial l^2})e_1 + (\frac{\partial W}{\partial l}\frac{\partial^2 U}{\partial l^2} - \frac{\partial U}{\partial l}\frac{\partial^2 W}{\partial l^2})e_2 \\ &+ (\frac{\partial U}{\partial l}\frac{\partial^2 V}{\partial l^2} - \frac{\partial V}{\partial l}\frac{\partial^2 U}{\partial l^2})e_3] + M_t(\frac{\partial U}{\partial l}e_1 + \frac{\partial V}{\partial l}e_2 + \frac{\partial W}{\partial l}e_3) \end{aligned} \tag{6}$$

A microelement section of the BHA is taken for analysis:

 doi:10.20944/preprints202604.0936.v1

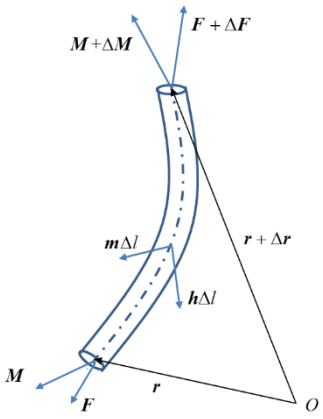

Figure 4. Schematic diagram of spatial deformation of microelement section

As shown in Figure 4, according to the moment balance principle for the BHA microelement section, the following equation is obtained:

$$(\boldsymbol{M}+\Delta M)-M+\boldsymbol{r}\times\boldsymbol{F}-(\boldsymbol{r}+\Delta r)\times(\boldsymbol{F}+\Delta F)+\boldsymbol{r}\times\boldsymbol{h}\Delta l=0 \tag{7}$$

Where: Δl is the length of the BHA microelement section; ΔM、Δr、ΔF are the variation of bending moment, displacement and internal force of the BHA microelement section, respectively; $\boldsymbol{h}$ is the external force vector per unit length of the drill string.

In statics analysis, the internal force and external force meet the balance relationship, which is expressed as:

$$\boldsymbol{h}\Delta l=\Delta F \tag{8}$$

By substituting Equation (8) into Equation (7) and dividing both sides by dl, the following equation is obtained:

$$\frac{\partial \boldsymbol{M}}{\partial l}+\boldsymbol{e}_t\times\boldsymbol{F}=0 \tag{9}$$

By substituting Equation (4) and Equation (6) into Equation (9), the following equation is obtained:

$$\begin{cases} EI\left(\dfrac{\partial V}{\partial l}\dfrac{\partial^3 W}{\partial l^3}-\dfrac{\partial W}{\partial l}\dfrac{\partial^3 V}{\partial l^3}\right)+M_t\dfrac{\partial^2 U}{\partial l^2}=F_y\dfrac{\partial W}{\partial l}-F_z\dfrac{\partial V}{\partial l} \\ EI\left(\dfrac{\partial W}{\partial l}\dfrac{\partial^3 U}{\partial l^3}-\dfrac{\partial U}{\partial l}\dfrac{\partial^3 W}{\partial l^3}\right)+M_t\dfrac{\partial^2 V}{\partial l^2}=F_z\dfrac{\partial U}{\partial l}-F_x\dfrac{\partial W}{\partial l} \\ EI\left(\dfrac{\partial U}{\partial l}\dfrac{\partial^3 V}{\partial l^3}-\dfrac{\partial V}{\partial l}\dfrac{\partial^3 U}{\partial l^3}\right)+M_t\dfrac{\partial^2 W}{\partial l^2}=F_x\dfrac{\partial V}{\partial l}-F_y\dfrac{\partial U}{\partial l} \end{cases} \tag{10}$$

The geometric constraint relationship is expressed as:

$$\left(\frac{\partial U}{\partial l}\right)^2+\left(\frac{\partial V}{\partial l}\right)^2+\left(\frac{\partial W}{\partial l}\right)^2=1 \tag{11}$$

Equation (11) is derived from the fact that the sum of squares of the included angles between the three sides and the diagonal of the microelement cube is 1.

It can be seen that the three equations in Equation (10) are not independent of each other. Based on different assumptions, the specific form of the three-dimensional mechanical model of the bottom hole assembly can be further derived.

For the BHA microelement section, the dynamic balance equation is expressed as:

 doi:10.20944/preprints202604.0936.v1

$$\frac{\partial^2(A\rho \boldsymbol{r})}{\partial t^2}=\frac{\partial \boldsymbol{F}}{\partial l}+\boldsymbol{h} \tag{12}$$

Where: A is the cross-sectional area of the drill string; ρ is the density of the drill string material; t is time.

It is assumed that the BHA is in a static state, so $\frac{\partial^2 \boldsymbol{r}}{\partial t^2}=0$. Only gravity and buoyancy are considered, and the following equation is obtained:

$$h=q\boldsymbol{k}=q\sin\alpha \boldsymbol{e}_1-q\cos\alpha \boldsymbol{e}_3 \tag{13}$$

Where: q is the buoyant weight per unit length of the drill string; $\boldsymbol{k}$ is the unit vector in the gravity direction (vertically downward), which can be decomposed into two directions: t (tangential) and n (normal); α is the well inclination angle.

By substituting Equation (13) into Equation (12) and integrating, the following equation is obtained:

$$\begin{aligned}\boldsymbol{F}&=F_x\boldsymbol{e}_1+F_y\boldsymbol{e}_2+F_z\boldsymbol{e}_3\\&=\boldsymbol{F}_0-\boldsymbol{e}_1\int_0^l q\sin\alpha dl-\boldsymbol{e}_3\int_0^l q\cos\alpha dl\\&=(S_x-ql\sin\alpha)\boldsymbol{e}_1+S_y\boldsymbol{e}_2+(ql\cos\alpha-B)\boldsymbol{e}_3\end{aligned} \tag{14}$$

Where: F0 is the internal force vector at the drill bit (l=0), which can be expressed as:

$$F_0=S_x\boldsymbol{e}_1+S_y\boldsymbol{e}_2-B\boldsymbol{e}_3 \tag{15}$$

Where: F_0 is the component of the drill string in the x direction at the drill bit; $F_{y0}$is the component of the drill string in the y direction at the drill bit; B is the pressure in the z direction of the drill string at the drill bit (i.e., WOB).

Then:

$$\begin{cases}F_x=S_x-ql\sin\alpha\\F_y=S_y\\F_z=-B+ql\cos\alpha\end{cases} \tag{16}$$

It is assumed that the deflection of the drill string is a small amount relative to its length, so the following relationship exists:

$$\frac{\partial W}{\partial l}=\sqrt{1-(\frac{\partial U}{\partial l})^2-(\frac{\partial V}{\partial l})^2}\approx 1 \tag{17}$$

By substituting Equation (17) into Equation (10) and ignoring high-order small quantities, the following equation is obtained:

$$\begin{cases}-EI\dfrac{\partial^3 V}{\partial l^3}+M_t\dfrac{\partial^2 U}{\partial l^2}=F_y-F_z\dfrac{\partial V}{\partial l}\\EI\dfrac{\partial^3 U}{\partial l^3}+M_t\dfrac{\partial^2 V}{\partial l^2}=F_z\dfrac{\partial U}{\partial l}-F_x\end{cases} \tag{18}$$

The longitudinal vibration and torsional vibration of the drill string are ignored, and only the lateral acceleration is considered (for the local drill string, the longitudinal acceleration is far less than the lateral acceleration and can be ignored). The following equation is obtained:

 doi:10.20944/preprints202604.0936.v1

$$\frac{\partial^2 \boldsymbol{r}}{\partial t^2} = \frac{\partial^2 U}{\partial t^2}\boldsymbol{e}_1 + \frac{\partial^2 V}{\partial t^2}\boldsymbol{e}_2 \tag{19}$$

It is assumed that the lateral resistance of the drilling fluid to the drill string is proportional to the lateral movement speed of the drill string. The following equation is obtained:

$$\begin{aligned} \boldsymbol{h} &= h_x\boldsymbol{e}_1 + h_y\boldsymbol{e}_2 + h_z\boldsymbol{e}_3 \\ &= (q\sin\alpha - C\frac{\partial U}{\partial t})\boldsymbol{e}_1 - C\frac{\partial V}{\partial t}\boldsymbol{e}_2 - q\cos\alpha\boldsymbol{e}_3 \end{aligned} \tag{20}$$

Where: C is the damping coefficient.

Therefore, by substituting Equation (19) and Equation (20) into the motion balance Equation (12), the following equation is obtained:

$$\frac{\partial \boldsymbol{F}}{\partial l} + h_x\boldsymbol{e}_1 + h_y\boldsymbol{e}_2 + h_z\boldsymbol{e}_3 = A\rho(\frac{\partial^2 U}{\partial t^2}\boldsymbol{e}_1 + \frac{\partial^2 V}{\partial t^2}\boldsymbol{e}_2) \tag{21}$$

By integrating Equation (21), the following equation is obtained:

$$\boldsymbol{F} + (ql\sin\alpha - S_x - Cl\frac{\partial U}{\partial t})\boldsymbol{e}_1 + (-S_y - Cl\frac{\partial V}{\partial t})\boldsymbol{e}_2 + (-ql\cos\alpha + \boldsymbol{B})\boldsymbol{e}_3 = A\rho l(\frac{\partial^2 U}{\partial t^2}\boldsymbol{e}_1 + \frac{\partial^2 V}{\partial t^2}\boldsymbol{e}_2) \tag{*}$$

Combined with Equation (4), the above equation can be written in component form:

$$\begin{cases} F_x = S_x + Cl\dfrac{\partial U}{\partial t} - ql\sin\alpha + \dfrac{\partial^2 U}{\partial t^2}A\rho l \\ F_y = S_y + Cl\dfrac{\partial V}{\partial t} + \dfrac{\partial^2 V}{\partial t^2}A\rho l \\ F_z = -B + ql\cos\alpha \end{cases} \tag{22}$$

It should be noted that for the equation（*）obtained after the integration of Equation (1.21), since $\boldsymbol{F}$ is also a vector, it corresponds to components in three directions (e1、e2 and e3). By expressing $\boldsymbol{F}$ in its component form, Equation (22) is derived.

By differentiating Equation (18) with respect to l and substituting the result into Equation (22), the following is obtained:

$$\begin{cases} A\rho\dfrac{\partial^2 U}{\partial t^2} = -EI\dfrac{\partial^4 U}{\partial l^4} - M_t\dfrac{\partial^3 V}{\partial l^3} + (ql\cos\alpha - B)\dfrac{\partial^2 U}{\partial l^2} + q\dfrac{\partial U}{\partial l}\cos\alpha + q\sin\alpha - C\dfrac{\partial U}{\partial t} \\ A\rho\dfrac{\partial^2 V}{\partial t^2} = -EI\dfrac{\partial^4 V}{\partial l^4} + M_t\dfrac{\partial^3 U}{\partial l^3} + (ql\cos\alpha - B)\dfrac{\partial^2 V}{\partial l^2} + q\dfrac{\partial V}{\partial l}\cos\alpha - C\dfrac{\partial V}{\partial t} \end{cases} \tag{23}$$

If the lateral vibration of the drill string is ignored, that is, the velocity term and acceleration term are not considered, the following conditions are met:

 doi:10.20944/preprints202604.0936.v1

$$\begin{cases} \dfrac{\partial U}{\partial t} = 0 \\ \dfrac{\partial V}{\partial t} = 0 \\ \dfrac{\partial^2 U}{\partial t^2} = 0 \\ \dfrac{\partial^2 V}{\partial t^2} = 0 \end{cases} \tag{24}$$

Then the three-dimensional small-deflection statics analysis differential equation of the bottom hole assembly can be obtained:

$$\begin{cases} EI\dfrac{\partial^4 U}{\partial l^4} = -M_t\dfrac{\partial^3 V}{\partial l^3} + (ql\cos\alpha - B)\dfrac{\partial^2 U}{\partial l^2} + q\dfrac{\partial U}{\partial l}\cos\alpha + q\sin\alpha \\ EI\dfrac{\partial^4 V}{\partial l^4} = M_t\dfrac{\partial^3 U}{\partial l^3} + (ql\cos\alpha - B)\dfrac{\partial^2 V}{\partial l^2} + q\dfrac{\partial V}{\partial l}\cos\alpha \end{cases} \tag{25}$$

1.2. Model Solution

Equation (25) has strong nonlinear characteristics and cannot be solved by the analytical method. Therefore, the numerical method is required to solve the three-dimensional small-deflection statics model of the bottom hole assembly. The BHA can be regarded as a beam with longitudinal and transverse bending, with the drill bit at the lower end and the tangent point at the upper end. It can be divided into n independent structural units by n-1 stabilizers and bending points. Spatial bending deformation of the BHA is generated under the loads of self-weight, WOB, torque, borehole wall support reaction force, and hydrostatic pressure of drilling fluid in the three-dimensional curved wellbore.

For the i-th section of the drill string, the wellbore axis coordinates at the upper end of the section are represented by $r_{oi} = X_i e_1 + Y_i e_2 + Z_i e_3$ (X, Y, Z are the coordinates of a point on the wellbore axis in the geodetic coordinate system); the drill string axis coordinates are represented by $r_i = U_i e_1 + V_i e_2 + W_i e_3$; the internal force of the drill string is represented by $F_i = F_{xi} e_1 + F_{yi} e_2 + F_{zi} e_3$; the external force per unit length of the drill string is represented by $h_i = q_i k$; the bending stiffness of the drill string is represented by $E_i I_i$; the torque on the drill string is represented by M_{ti} . By discretizing Equation (25), the differential equations for three-dimensional small-deflection statics analysis of BHA are obtained:

$$\begin{cases} E_i I_i U_i'''' = -M_{ti} V_i''' + (q_i l\cos\alpha_i - B_i)U_i'' + q_i U_i'\cos\alpha_i + q_i\sin\alpha_i \\ E_i I_i V_i'''' = M_{ti} U_i''' + (q_i l\cos\alpha_i - B_i)V_i'' + q_i V_i'\cos\alpha_i \end{cases} \tag{26}$$

According to Equation (18) and Equation (22), the lateral force on the BHA unit is obtained as:

$$\begin{cases} F_{xi} = -E_i I_i U_i''' - M_{ti} V_i'' + (q_i l\cos\alpha_i - B_i)U_i' \\ F_{yi} = -E_i I_i V_i''' + M_{ti} U_i'' + (q_i l\cos\alpha_i - B_i)V_i' \end{cases} \tag{27}$$

 doi:10.20944/preprints202604.0936.v1

$$\begin{cases} (\ )' = \dfrac{d(\ )}{dl}, (\ )'' = \dfrac{d^2(\ )}{dl^2}, (\ )''' = \dfrac{d^3(\ )}{dl^3}, (\ )'''' = \dfrac{d^4(\ )}{dl^4} \\ B_i = B_1 - \sum_{j=1}^{i-1}(q_j L_j \cos\alpha_j - N_j f_a), M_{ti} = M_{t1} - \dfrac{f_t D_w}{2}\sum_{j=1}^{i-1} N_j \\ f_a = \dfrac{2vf}{\sqrt{4v^2 + (wD_w)^2}}, f_t = \dfrac{wD_w f}{\sqrt{4v^2 + (wD_w)^2}} \end{cases} \tag{28}$$

The meaning of each parameter in the formula is as follows:

l — Curve coordinate along the drill string axis;

E_i — Elastic modulus of the i-th drill string section;

I_i — Section moment of inertia of the i-th drill string section;

M_{ti} — Torque on the i-th drill string section;

q_i — Linear weight of the i-th drill string section in drilling fluid;

α_i — Well inclination angle of the well section where the i-th drill string section is located;

U_i'' — Displacement/coordinate of the i-th drill string section in the x direction;

V_i' — Displacement/coordinate of the i-th drill string section in the y direction;

B_i — Pressure in the lower z direction of the i-th drill string section;

L_j — Length of the j-th drill string section;

N_j — Contact pressure between the j-th stabilizer and the borehole wall;

f — Friction coefficient between the stabilizer and the borehole wall;

v — Drilling ROP;

w — Rotation angular velocity of the drill string;

D_w — Wellbore diameter.

1.2.1. Boundary Conditions and Continuity Conditions

(1) At the drill bit: The displacement of the drill bit is zero, and no bending moment exists between the drill bit and the formation.

$$[U_1(0)]^2 + [V_1(0)]^2 + [U''_1(0)]^2 + [V''_1(0)]^2 = 0 \tag{29}$$

(2) At the stabilizer:

(a) Contact with the well wall. The displacement and its first derivative and the bending moment of the drill string on stabilizer's both sides are continuous is continuous.

$$\begin{cases} U_i(L_i) = U_{i+1}(0) = X_i + e_{ci}\cos\delta_i \\ V_i(L_i) = V_{i+1}(0) = Y_i + e_{ci}\sin\delta_i \\ U_i'(L_i) = U_{i+1}'(0) \\ V_i'(L_i) = V_{i+1}'(0) \\ EIU_i''(L_i) = E_{i+1}I_{i+1}U_{i+1}''(0) \\ EIV_i''(L_i) = E_{i+1}I_{i+1}V_{i+1}''(0) \end{cases} \tag{30}$$

Where, 0 represents the starting point of this section; Li represents the terminal point of this section. e_{ci} is eccentricity; δ_i is deflected angle of the stabilizer; X_i is x-coordinate of the wellbore

 doi:10.20944/preprints202604.0936.v1

axis at the stabilizer or contact point; Y_i is y-coordinate of the wellbore axis at the stabilizer or contact point.

(b) Not contact with the well wall. The drill string coordinates on both sides of the stabilizer are continuous, and its derivative continuous, moment continuous, and internal force continuous.

$$\begin{cases} U_i(L_i) = U_{i+1}(0) \\ V_i(L_i) = V_{i+1}(0) \\ U_i^{'}(L_i) = U_{i+1}^{'}(0) \\ V_i^{'}(L_i) = V_{i+1}^{'}(0) \\ EIU_i^{''}(L_i) = E_{i+1}I_{i+1}U_{i+1}^{''}(0) \\ EIV_i^{''}(L_i) = E_{i+1}I_{i+1}V_{i+1}^{''}(0) \\ F_{xi}(L_i) = F_{xi+1}(0) \\ F_{yi}(L_i) = F_{yi+1}(0) \end{cases} \tag{31}$$

(3) At the tangent point: The slope and curvature at the tangent point are consistent with those of the wellbore axis.

$$\begin{cases} U_n(L_n) = X_n + (D_w - D_{on})/2 \\ V_n(L_n) = Y_n \\ U^{'}{}_n(L_n) \approx X^{'}{}_n \\ V^{'}{}_n(L_n) \approx Y^{'}{}_n \\ U^{''}{}_n(L_n) \approx X^{''}{}_n \\ V^{''}{}_n(L_n) \approx Y^{''}{}_n \end{cases} \tag{32}$$

Where, D_{on} is outer diameter of the drill string at the tangent point.

(4) Wellbore constraint: The deformation of the drill string is restricted by the wellbore, and it must be satisfied for any point.

$$\sqrt{(U_i - X)^2 + (V_i - Y)^2} \le (D_w - D_{oi})/2 \tag{33}$$

Where, D_{oi} is outer diameter of the i-th drill string unit.

(5) bend angle position: If there is a bend angle on the i-th section of the drill string, which is positioned between the (i-1)th stabilizer and the i-th stabilizer, splitting this section of the drill string into two parts. The bend angles and the tool face angles of the two parts are θ_{i1} and ω_{i1} respectively, and the lengths of the two parts are L_{i1} and L_{i2} respectively. Then, in accordance with the adjacent function theorem, the displacement continuity condition between the two parts are:

$$U_{i2} = U_{i1} - \frac{\sin\theta_{i1}\cos\omega_{i1}\sin[k_i(l - L_{i1})]}{k_i} \tag{34}$$

$$V_{i2} = V_{i1} - \frac{\sin\theta_{i1}\sin\omega_{i1}\sin[k_i(l - L_{i1})]}{k_i} \tag{35}$$

Where, $k_i = \sqrt{\frac{B_i + B_{i+1}}{2EI}}$.

1.2.2. Weighted Residual Method for Solving the BHA Three-dimensional Mechanical Model

 doi:10.20944/preprints202604.0936.v1

The weighted residual method is adopted[20]. By assuming the piecewise displacement trial function, the numerical solution of Equation (25) can be obtained. In this section, a simple BHA structure with two units and a single stabilizer (i.e., drill bit - stabilizer - upper tangent point, see Figure 5) is taken as an example to illustrate the solution process of the weighted residual method. In the weighted residual method, the selection of the trial function is crucial. It must be continuous and complete, and meet the requirements of boundary conditions and convergence.

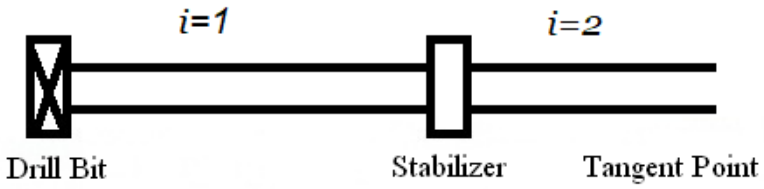

Figure 5. Schematic diagram of the simple BHA structure of drill bit - stabilizer - upper tangent point.

For a structure with two units and three nodes, the displacement trial function can be selected in the form of a quartic polynomial:

$$\begin{cases} U_i = \sum_{r=0}^{s} a_{ir} l^r \\ V_i = \sum_{r=0}^{s} b_{ir} l^r \end{cases} \tag{36}$$

S represents the degree of the highest term. When S = 4, the displacement trial function can be expressed as:

$$\begin{cases} U_i = a_{i0} + a_{i1} l + a_{i2} l^2 + a_{i3} l^3 + a_{i4} l^4 \\ V_i = b_{i0} + b_{i1} l + b_{i2} l^2 + b_{i3} l^3 + b_{i4} l^4 \end{cases} \tag{37}$$

By substituting the boundary conditions and solving the coefficients jointly, the lateral force of the drill bit at a certain moment when the tool face angle of the pre-bent anti-tilt BHA is ω can be ultimately solved:

$$F_\alpha = E_1 I_1 U_1''' \ (0) + M_{ti} V_1'' \ (0) + B_1 U_1' \ (0) \tag{38}$$

$$F_\varphi = -E_1 I_1 V_1''' \ (0) + M_{ti} U_1'' \ (0) - B_1 V_1' \ (0) \tag{39}$$

The combined guiding force of the drill bit of the pre-bent anti-deviation BHA (such as the BHA with a single-bent motor) driven by the ground rotary can be represented by the resultant force F_s of the lateral forces of the drill bit corresponding to the constantly changing tool face angle.

When the BHA rotates for one cycle, the value range of ω is $0 - 2\pi$. Let the number of calculation points be n, then the change step of the tool face angle is $\Delta\omega = 2\pi/n$. At this moment, the combined guiding force F_s can be expressed as:

$$F_s = \frac{1}{n} \sqrt{F_{s\alpha}{}^2 + F_{s\phi}{}^2} \tag{40}$$

Where, $F_{s\alpha}$ is resultant force on well inclination plane, $F_{s\alpha} = \sum_{\omega=0}^{2\pi} F_{\alpha(\omega)}$; $F_{s\varphi}$ is resultant force on well azimuthal plane, $F_{s\varphi} = \sum_{\omega=0}^{2\pi} F_{\varphi(\omega)}$; The direction angle of the combined guiding force (the included angle between the combined guiding force and the high side) is:

$$\alpha_s = \arctan(F_{s\phi} / F_{s\alpha}) \tag{41}$$

 doi:10.20944/preprints202604.0936.v1

2. Analysis of Calculation Results for Deviation-reducing Force

2.1. Pre-bent Anti-deviation Drilling Tool Assembly

The 311.2 mm wellbore section is analyzed. A pre-bent anti-deviation drilling tool assembly (Figure 6) is assumed to be used. The configuration is determined: 311.2 mm PDC bit + 244.475 mm motor (bend angles: 0.75°, 1°, 1.15°; 308 mm stabilizer) + 228.6 mm DC + 311 mm stabilizer + drill pipes.

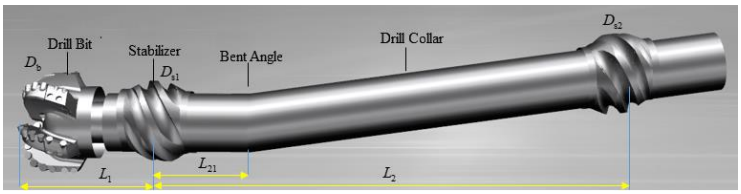

Figure 6. Pre-bent anti-deviation drill string assembly and parameters.

The calculation parameters are defined: L_{21} is 1.235 m, L1 is 1.172 m, and L2 is 18.3 m

L_1 is defined as the distance from the drill bit to the near-bit stabilizer. L_{21} is defined as the distance from the motor bend to the near-bit stabilizer. L_2 is defined as the distance from the near-bit stabilizer to the upper stabilizer.

(1) The force conditions on the drill bit were calculated for bend angles of 0.75°, 1°, and 1.15°. As can be observed from Figure 7, the forces exerted on the drill bit in all directions are increased as the bend angle increases. However, a consistent mushroom-like shape is maintained by all force profiles. The resultant steering force of the drill bit is also increased with the bend angle. When the bend angle is 1.15°, a deviation reduction force of 19.68 kN is achieved. The force direction is 178.82°, pointing towards the lower wellbore wall. Good anti-deviation effects are exhibited.

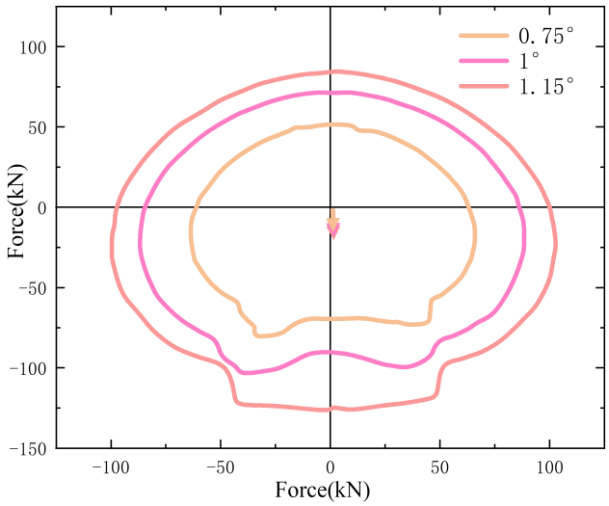

Figure 7. Force distribution on the drill bit and deviation reduction force.

The deviation reduction force on the drill bit was calculated for bend angles ranging from 0.5° to 1.5°. The influence law of the bend angle on the deviation reduction force was analyzed. It is indicated in Figure 8 that the deviation reduction force is increased as the bend angle of the pre-bent assembly increases from 0.5° to 1.13°. When the bend angle is further increased from 1.13° to 1.5°, an overall decreasing trend is presented by the deviation reduction force. A larger deviation reduction force is generated by the drill bit when the bend angle is within the range of 1° to 1.13°. The direction of the deviation reduction force is stabilized near 180°.

 doi:10.20944/preprints202604.0936.v1

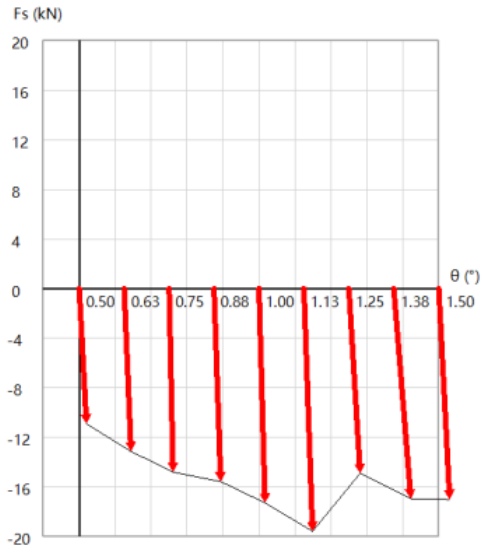

Figure 8. Variation law of the bit deviation reduction force with the bend angle.

(2) Effect of L_1 on Deviation Reduction Force

The deviation reduction force on the drill bit was calculated for different distances between the near-bit stabilizer (on the motor) and the drill bit, under bend angles of 0.75°, 1°, and 1.15°. As shown in Figure 9, a larger deviation reduction force is produced when the near-bit stabilizer is positioned closer to the drill bit. The deviation reduction force is rapidly decreased as L_1 increases. The force gradually becomes stable after L_1 exceeds 1.5 m. When L_1 is constant, the deviation reduction force is increased as the bend angle increases. However, this distance is generally controlled at approximately 1 m during actual manufacturing.

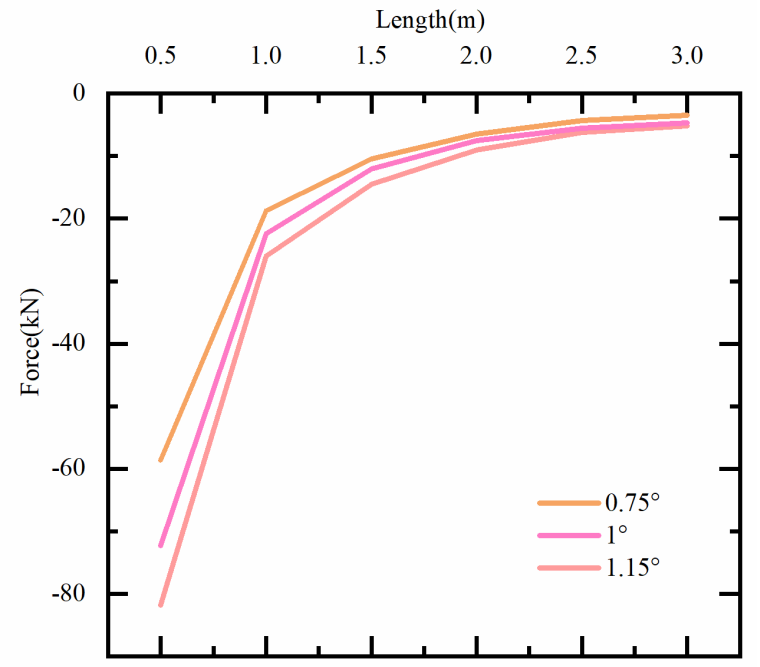

Figure 9. Variation law of the bit deviation reduction force with L_1.

(3) Effect of L_2 on Deviation Reduction Force

Effect of L_2 on Deviation Reduction Force The deviation reduction force on the drill bit was calculated for different upper stabilizer positions, under bend angles of 0.75°, 1°, and 1.15°. It can be seen from Figure 10 that irregular variations are exhibited by the deviation reduction force as L_2

 doi:10.20944/preprints202604.0936.v1

increases. When the bend angle is 0.75°, the deviation reduction force first increases and then decreases with the increase of L_2. The maximum force and best anti-deviation effect are achieved when L_2 is 10 m. When the bend angle is 1°, a decreasing trend is presented by the deviation reduction force as L_2 increases, and the force is maximized at an L_2 of 5 m. When the bend angle is 1° (as stated in the source text), the force first decreases and then increases with L_2, achieving a maximum at an L_2 of 5 m.

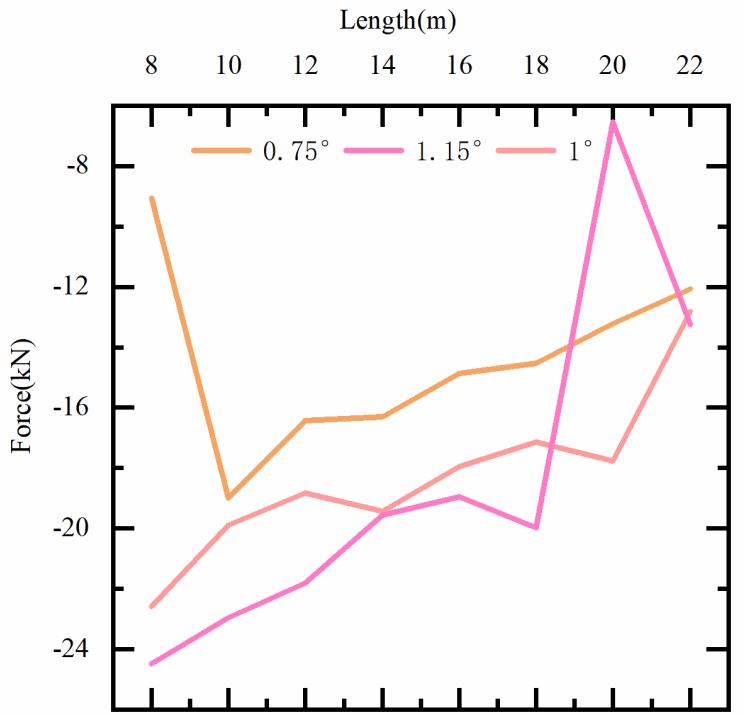

Figure 10. Variation law of the bit deviation reduction force with L_2.

(4) Effect of Upper Stabilizer Diameter on Deviation Reduction Force

The deviation reduction force was calculated for different upper stabilizer diameters, under bend angles of 0.75°, 1°, and 1.15°. As observed in Figure 11, an overall increasing trend in the deviation reduction force is presented as the upper stabilizer diameter increases. When the near-bit stabilizer diameter is constant, the deviation reduction force is significantly increased with a larger bend angle.

 doi:10.20944/preprints202604.0936.v1

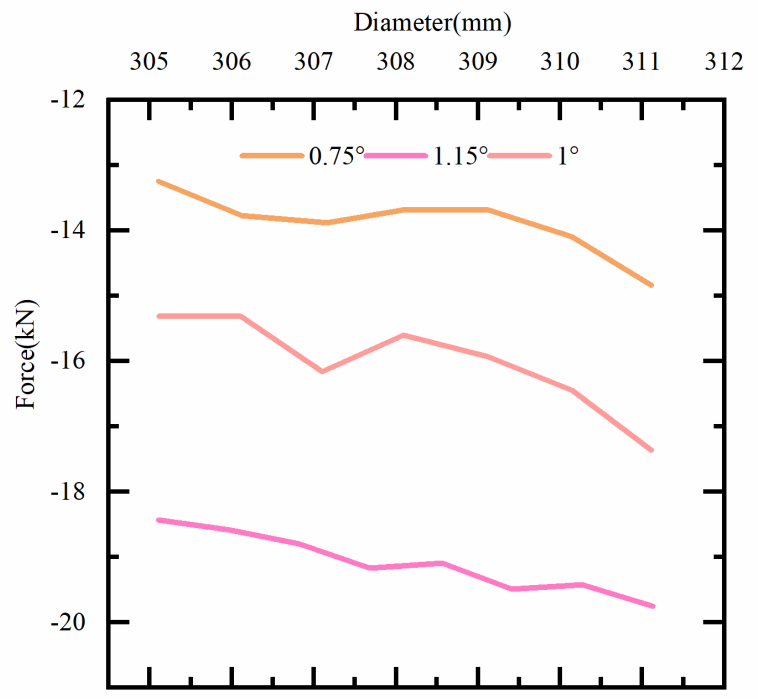

Figure 11. Variation law of the bit deviation reduction force with the upper stabilizer diameter.

(5) Effect of Upper Stabilizer Diameter on Deviation Reduction Force

The deviation reduction force was calculated for different upper stabilizer diameters, under bend angles of 0.75°, 1°, and 1.15°. As observed in Figure 12, an overall increasing trend in the deviation reduction force is presented as the upper stabilizer diameter increases. When the near-bit stabilizer diameter is constant, the deviation reduction force is significantly increased with a larger bend angle.

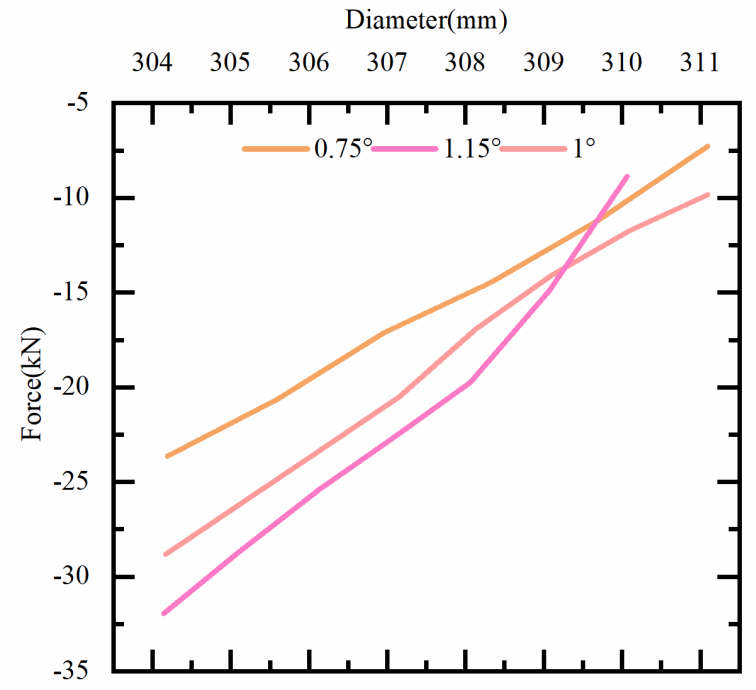

Figure 12. Variation law of the bit deviation reduction force with the upper stabilizer diameter.

2.2. Conventional Pendulum Drill String Assembly

 doi:10.20944/preprints202604.0936.v1

A conventional pendulum assembly was also evaluated. The configuration is as follows: Φ311.2 mm PDC bit × 0.35 m + Φ228.6 mm DC × 19 m + Φ311 mm stabilizer × 1.95 m + drill pipe. The calculation parameter was set as L1 = 20.3 m. For a conventional pendulum, only a minimal deviation reduction force can be provided to the drill bit, which is demonstrated in Figure 13.

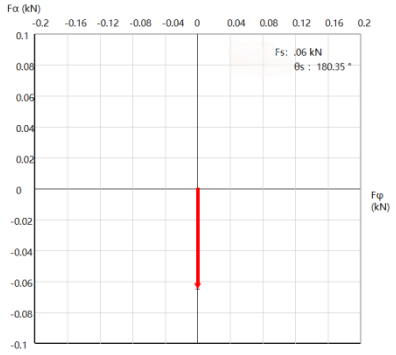

Figure 13. Deviation reduction force of the conventional pendulum assembly.

The influence law of the stabilizer size is illustrated in Figure 14. Because the generated deviation reduction force is extremely small, the effect of different stabilizer outer diameters is almost negligible.

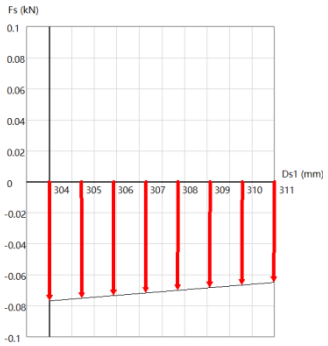

Figure 14. Influence law of the stabilizer size.

As can be seen from Figure 15, the distance from the drill bit to the stabilizer must exceed 18 m for a deviation reduction effect to be achieved by this assembly.

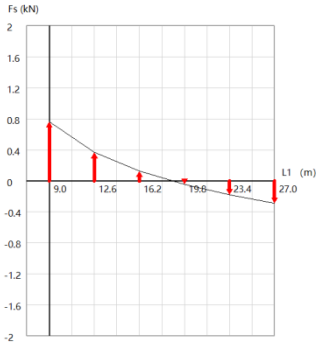

Figure 15. Influence law of the distance from the stabilizer to the drill bit.

Based on the comprehensive analysis, a difference of over two orders of magnitude in the resultant steering force is observed between the pre-bent assembly and the conventional pendulum assembly. Therefore, excellent anti-deviation and straightening effects are possessed by the pre-bent assembly.

 doi:10.20944/preprints202604.0936.v1

2.3. Drill String Assembly Optimization

The drill string assembly was optimized primarily based on the deviation reduction force. Previously, a 0.75° motor was commonly used for drilling 12.25-inch wellbores in the Bohai Oilfield, as illustrated in Figure 13. Since a larger deviation reduction force is generated when the motor bend angle is between 1° and 1.13°, the motor bend angle was optimized from 0.75° to 1.15°. In the original assembly, two drill collars were connected above the motor, and the distance between the motor stabilizer and the upper stabilizer exceeded 20 m. Based on the previous calculations, the best anti-deviation effect is achieved when this distance is 10 m. Therefore, the connection was optimized from two drill collars to a single short drill collar (1~3 m), reducing the distance between the two stabilizers to approximately 9~11 m (Figure 16). Simultaneously, the distance from the drill bit to the motor sleeve was shortened from 1.2 m to 0.9 m, and the motor stabilizer diameter was reduced from 308 mm to 305 mm.

Figure 16. Motor drilling application in the Bohai Oilfield.

3. Field Application

Complex geological conditions are found in a specific block of the Bohai Oilfield. It was indicated by adjacent wells that well deviation is highly prone to occur during drilling, with maximum deviations exceeding 8° in multiple adjacent wells. To ensure wellbore quality and achieve anti-deviation in the 12 1/4-inch section of Well X-4, a motor (0°/308 mm) combined with Power V was utilized in the upper section (two trips), and a torsional impact drilling tool combined with Power V was used in the lower section (one trip). A total of three trips were required. The well depth ranged from 2192.00 to 4265.00 m, a maximum drilling pressure of 10 t was applied, and a maximum deviation of 1.84° was recorded.

In Well X-6, the pre-bent drill string assembly was designed and utilized. The detailed assembly was structured as follows: 12-1/4" PDC-BIT + 9-5/8" motor (1.15°/305 mm) + 9" DC + X/O + 12-1/8" STB + 8" F/V + 8" DC × 3 + vertical well surveying tool + 8" DC × 3 + 8" (F/J+JAR) + LWD plugging sub + X/O + 5-1/2" HWDP × 14. The actual drilled depth ranged from 2302.00 to 4180.00 m. A maximum drilling pressure of 13 t was applied, and a maximum deviation of 3.26° was observed, which met the quality specification requirements for the wellbore.

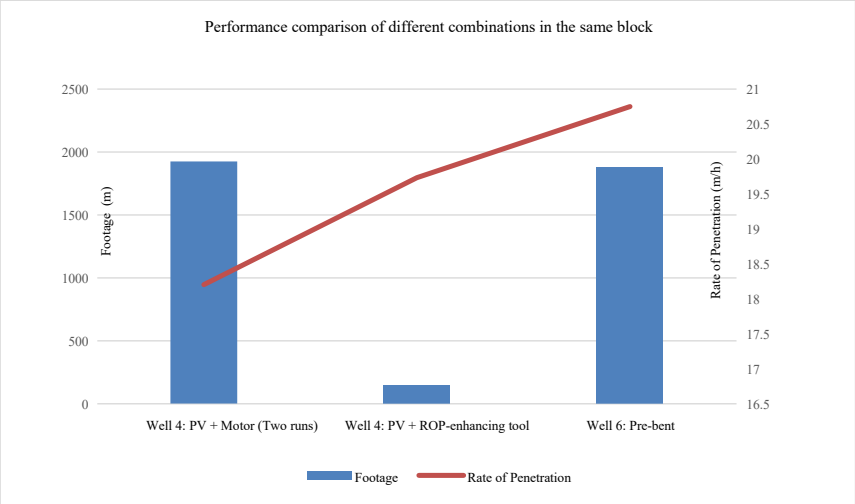

Figure 17. Comparison chart of the rate of penetration (ROP).

 doi:10.20944/preprints202604.0936.v1

During the actual drilling process, as illustrated in Figure 17, a footage of 1878 m was completed in a single trip using the pre-bent assembly under roughly the same well depth. Excellent anti-deviation effects were achieved. Furthermore, a certain advantage in the rate of penetration (ROP) is still maintained compared to the Power V (PV) assembly, realizing an overall ROP increase of approximately 14%. A cost saving of approximately 1.5 million RMB per well operation is achieved. Assuming an annual application of 50 wells, an estimated 75 million RMB could be saved annually.

The anti-deviation and speed-increasing technology of the pre-bent assembly has been trialed since December 2023. In 2024, it was comprehensively promoted in 12.25-inch wellbores and applied in deep 16-inch and 8.5-inch piedmont wellbore sections. In the applied 12.25-inch wellbore sections, among the 22 wells, deviations exceeding 2° were recorded in 4 wells, deviations between 1° and 2° in 11 wells, and deviations between 0° and 1° in the remaining 7 wells. The maximum deviation was 2.46°, and all wellbore quality specification requirements were met. It is demonstrated by field practices that excellent anti-deviation and speed-increasing effects are provided by the pre-bent assembly. Currently, Power V tools have been fundamentally replaced by this technology in vertical well piedmont formations of the Bohai Sea in China.

4. Conclusions and Suggestions

(1) Critical parameters of the pre-bent BHA were computationally analyzed. It was found that the deviation reduction force first increases and then decreases with the bend angle. The force is maximized when L1 is smaller, the near-bit stabilizer diameter is smaller, and the upper stabilizer diameter is larger.

(2) For conventional pendulum assemblies, the stabilizer diameter has almost no effect on the deviation reduction force. The pre-bent assembly provides a deviation reduction force that is advantageous by more than two orders of magnitude.

(3) Based on the results, an optimized pre-bent assembly was designed with a bend angle of 1.15°, a near-bit stabilizer diameter of 305 mm, an L1 of 0.9 m, and an L2 of 9 to 11 m.

(4) Field applications across 22 exploration wells show that the pre-bent assembly provides strong anti-deviation effects, allows full release of drilling pressure, and increases drilling speed by about 14% while saving significant trips and costs.

(5) In the future, this tool combination can be promoted to wellbores of other sizes. By optimizing customized bend angles, all-metal motors, and impregnated bits, a suite of pre-bent assemblies specifically suited for buried-hill formations in the Bohai Sea can be developed.

Funding: This research was funded by the National Key Research and Development Program of China, grant number 2022YFC2806100; the National Natural Science Foundation of China, grant numbers U22B20126 and 52504012.

Data Availability Statement: The original contributions presented in this study are included in the article. Further inquiries can be directed to the corresponding author.

Conflicts of Interest: Authors Li Wenlong, Li Zhuangwei, Xi Jiangjun, Jin Nan, and Cheng long were employed by the Tianjin Branch of CNOOC Ltd. The remaining authors declare that the research was conducted in the absence of any commercial or financial relationships that could be construed as a potential conflict of interest.

References

1. Deng, Y. Formation mechanism and exploration practice of large-medium buried-hill oil fields in Bohai Sea. Acta Pet. Sin. 2015, 36. DOI: 10.7623/syxb201503001
2. Xu, C.; Zhou, J.; Yang, H.; Guan, D.; Su, W.; Ye, T.; Zhao, D. Discovery of large-scale metamorphic buried-hill oilfield in Bohai Bay Basin and its geological significance. Acta Petrolei Sinica 2023, 44, 1587. DOI: 10.7623/syxb202310001
3. Hou, M.; Cao, H.; Li, H. Characteristics and controlling factors of deep buried-hill reservoirs in the BZ19-6 structural belt, Bohai Sea area. Natural Gas Industry B 2019, 6, 305–316. https://doi.org/10.1016/j.ngib.2019.01.011

 doi:10.20944/preprints202604.0936.v1

4. Ye, T.; Niu, C.; Wei, A. Characteristics and genetic mechanism of large granitic buried-hill reservoir, a case study from PengLai oil field of Bohai Bay Basin, north China. Journal of Petroleum Science and Engineering 2020, 189, 106988. https://doi.org/10.1016/j.petrol.2020.106988
5. Wang, H.; Su, Y. Progress of theoretical research on deviation control and drilling fast for vertical wells. Acta Petrolei Sinica 2004, 25, 86. DOI: 10.7623/syxb200403018
6. Ghosh, S. A review of basic well log interpretation techniques in highly deviated wells. Journal of Petroleum Exploration and Production Technology 2022, 12, 1889–1906. https://doi.org/10.1007/s13202-021-01437-2
7. Zou, W.; Chen, S. Hazards and preventive measures of well deviation in well construction of in-situ leaching. Uranium Mining and Metallurgy 2006, 25. https://www.osti.gov/etdeweb/biblio/20945348
8. Al Hajeri, M.; Al Safar, W.; Gupta, P.K.; Raturi, S.K.; Al Zankawi, O.; Bojarah, K.H.; Al Ghareeb, A.Y.; Al Aryan, A.M.; Naik, V.; Shastri, M.C.; Belhouchet, M.; Abdessalem, A. Wellbore stability management to avoid serious drilling hazards in high deviated well-application of real time geomechanics. In Proceedings of the Abu Dhabi International Petroleum Exhibition and Conference, SPE: Abu Dhabi, UAE, 2017; D031S071R006. https://doi.org/10.2118/188329-MS
9. Foroud, T.; Dehkordi, B.K. Well deviation problem: A case study in an Iranian gas well drilling. International Journal of Petroleum Technology 2020, 7, 7–19. https://doi.org/10.15377/2409-787X.2020.07.2
10. Wang, D.; Zhang, W.; Zhang, X. Well-deviation control techniques for strong dipping strata. In The China Continental Scientific Drilling Project: CCSD-1 Well Drilling Engineering and Construction; Springer: Berlin/Heidelberg, Germany, 2015; pp. 233–272. https://doi.org/10.1007/978-3-662-46557-8_8
11. Gao, D. Discussion on theory and technology of deviation control and fast drilling in deviation-prone formations. Petroleum Drilling Techniques 2005, 19–22. https://kns.cnki.net/kcms2/article/abstract?v=m07J8nP_wCFPfEv4fTmM84WsLpWIhq9pipu9AbFAxpiWlbQvAj0KzLzS73X6DyAUN95_hfoq6vp8hUcwMWbfvTMwTx-nm-xP27J-doPfakme0uY9TheBp9CFc2AVwAg0fzfBcekXvTh_4acq-NKxrKeaPzWAlV1Wc8Qkc-f6sAhquISvLAJA4w==&uniplatform=NZKPT&language=CHS
12. Gao, D.; Huang, W. Several research progress and development suggestions on theory and technology of ultra-deep well engineering. Petroleum Drilling Techniques 2024, 52, 1–11. DOI:10.11911/syztjs.2024024
13. Yin, Z.; Bai, J.; He, J. A review of bottom hole assemblies for vertical well deviation control. Natural Gas Industry 2000, 20, 50–53. https://kns.cnki.net/kcms2/article/abstract?v=m07J8nP_wCGLhiep8U40lN2bADXoaZpJP35Sm_RFK54wEF4Kkm02PsqM8B_pWImbql_SfBbAq3E-XlZUaoCPOm0722S13QK17zerDGXDS-kal7qEfWXqI-z6RQxpCeJnWXojWvE4pk1sDn-e7n_1NZ4ndyRZlsGTcdpBGov-O4aPX75kYvlkuw==&uniplatform=NZKPT&language=CHS
14. Xu, Y.; Wang, L.; Chen, X.; Fan, Y. Improvement of drilling quality using precision directional drilling technology. Journal of Petroleum Exploration and Production Technology 2022, 12, 3149–3164. https://doi.org/10.1007/s13202-022-01510-4
15. Wang, W.; Zhang, H.; Li, N.; Wang, C.; Teng, X.; Zhu, W.; Di, Q. The dynamic deviation control mechanism of the prebent pendulum BHA in air drilling. Journal of Petroleum Science and Engineering 2019, 176, 521–531. https://doi.org/10.1016/j.petrol.2019.01.008
16. Zhang, H.; Di, Q.; Wang, W.; Chen, F.; Chen, W. Lateral vibration analysis of pre-bent pendulum bottom hole assembly used in air drilling. Journal of Vibration and Control 2018, 24, 5213–5224. https://doi.org/10.1177/1077546317747778
17. Di, Q.; Wu, Y.; Shi, X. Preliminary study on pre-bending dynamic deviation control and fast drilling technology. Acta Petrolei Sinica 2003, 86–89. https://kns.cnki.net/kcms2/article/abstract?v=m07J8nP_wCF3SZtgyh50iFCAWlXSY0P62KD6J2DG31VhC7RPQPjTFYytwTUTyWryJrzqvYEVzogD9ao7001QwjChrWmhI7--61ChtOt72IKmUmP29B8V7D3K2bPXsnh4e0I8FvAskzWwDqQYiGE4jxu7giOq-3EwT3nNaSYZsNt4BlKRwJsu-g==&uniplatform=NZKPT&language=CHS
18. Di, Q.; Hu, F.; Zhou, B.; Wang, W. Dynamic behavior of pre-bent pendulum assembly for deviation control in air drilling. Natural Gas Industry 2019, 39, 94–98. DOI: 10.3787/j.issn.1000-0976.2019.07.012

 doi:10.20944/preprints202604.0936.v1

19. Wang, H.; Dong, S. Simulation model for lateral vibration of axially reciprocating sucker rod string in a curved wellbore. Engineering Mechanics 2020, 37, 228–237. DOI: 10.3787/j.issn.1000-0976.2019.07.012
20. Xu, W. Analysis of dynamic problems by weighted residual method. Journal of Southwest Jiaotong University 1982, 3. https://kns.cnki.net/kcms2/article/abstract?v=m07J8nP_wCEH07NCP3PLan69k6IRrZ9wfhNoaTKbzqJQOu_SmryFL5omI7WhvQVh7kpm3c3QEQAil97ccDWQIdKffvq_JdS8a4v3CIqdpKU0IJwHpPZYfgX-QeiUkd56e-Drp45hC4baJd2PRLTHnVb5oJ86xc6TcvYCNABHAcX5Bhp2Div-Qg==&uniplatform=NZKPT&language=CHS